Efficient and Optical Feedback Tolerant Hybrid Laser Design for Silicon Photonics Applications

Lorenzo Columbo, Jock Bovington, *Member, IEEE*, Sebastian Romero-Garcia, Dominic F. Siriani, and Mariangela Gioannini

***Abstract*—We present a design of a tunable hybrid laser based on III-V Reflective Semiconductor Optical Amplifier (RSOA) and Silicon Photonics (SiPh) external mirror that represents a good trade off between high Wall-Plug Efficiency (WPE) and high tolerance to optical feedback caused by unwanted back reflections from the rest of the SiPh chip. The sensitivity to optical feedback of different configurations, an important issue in many SiPh applications, is evaluated through the calculation of the critical feedback level based on an effective Lang-Kobayashi model and the main results are validated through numerical simulations of laser dynamics. We conclude that hybrid lasers with long effective external cavities typically designed to reduce the laser linewidth can be also exploited to improve the tolerance to spurious optical feedback.**

***Index Terms*—Hybrid lasers, silicon photonics, optical feedback.**

I. Introduction

THE field of silicon photonic technologies has found in the last years a significant boost triggered by the industrial interest for the development of low cost and mass production optical devices for many fields of application [1]; one in particular is the development of optical transceivers for data center interconnects [2]. Concerning optical transmitters an important issue is the integration of the laser source with the rest of the silicon photonics integrated circuit (SiPh PIC); the first challenge is the selection of the most reliable technology for the integration of the III-V gain material (hybrid integration [3], heterogeneous bonding [4] or epitaxial growth on silicon [5]) and the second is the development of lasers tolerant to the external optical feedback. The integration of an optical isolator in silicon is indeed still considered of too low performance for the industrial market. Main reasons are the need of bonding a magneto-optic garnet that causes high optical insertion loss [6], the use of ring based structures that limit the isolator optical bandwidth [7], or the implementation of quite complex and difficult to control topologies [8]. This motivates the recent efforts in designing laser sources as much tolerant as possible to optical feedback. In fact in any SiPh PIC the coherent light might be reflected back into the laser from the rest of the PIC due to any optical waveguide mismatch (at a distance of maximum few centimeters) or by the optical output coupling fiber (at distances of several centimeters). Up to now, only quantum dots lasers either edge-coupled to the SiPh PIC or epitaxially grown on silicon have shown much higher tolerance to optical feedback respect to the Multi Quantum Well (MQW) counterpart [9], [10], [11], [12]. In the case of quantum dash it has been very recently shown that high robustness with respect to optical feedback is obtained for nanostructures oriented perpendicular to the cavity axis associated with a smaller linewidth enhancement factor [13]. MQW distributed feedback laser diodes edge-coupled to SiPh PIC are not a viable solution in this context because they start to be unstable at optical feedback level starting from −40 dB [9]. An original ring configuration with weak optical isolation, which guarantees unidirectional operation, has been proposed as candidate to increase the feedback tolerance of integrated semiconductor lasers based on MQW [14], although the current design sensitivity to external feedback is comparable to that of a standard Fabry-Perot laser.

In this work we consider hybrid lasers realized via the edge-coupling of a commercial MQW HR/AR reflective SOA (RSOA, providing the III-V gain material) with a SiPh PIC designed as the front mirror of the laser cavity [15], [16], [17], [18]. The high flexibility in the design of the SiPh mirror with micro-ring resonators has allowed the realization of lasers with high wall-plug efficiency (WPE) or the development of widely tunable and very narrow linewidth lasers exploiting the long effective length of the external cavity obtained by these compact mirrors [15], [17]–[19]. The silicon nitride (SiN) waveguides are particularly promising at this purpose [17] thanks to the very low losses and low non-linear effects when compared with silicon waveguides. Most of the literature also shows that hybrid lasers with narrow linewidth typically emit low power with low WPE: for example an optical linewidth of 37 kHz at 11 mW output power with WPE of only 4.4% is demonstrated in [18], while a linewidth of 65 kHz and 16 mW output power is reported in [20], but at the cost of very high SOA bias current of 500 mA and thus low WPE. Those designs that have maximized the WPE [16] did not set specific requirements on the optical linewidth.

To the best of our knowledge, a detailed study about the tolerance to optical feedback of these hybrid lasers has not been

Manuscript received June 14, 2019; revised September 17, 2019; accepted September 27, 2019. Date of publication October 7, 2019; date of current version November 6, 2019. *(Corresponding author: Mariangela Gioannini.)* This work was supported by the CISCO Sponsored Research Agreement TOSCA (Detectors and Sources for Silicon Photonic Integrated Circuits in the CISCO platform).

L. Columbo and M. Gioannini are with the Dipartimento di Elettronica e Telecomunicazioni, Politecnico di Torino, 10129 Torino, Italy (e-mail: lorenzo.columbo@polito.it; mariangela.gioannini@polito.it).

J. Bovington, S. Romero-Garcia, and D. F. Siriani are with the Cisco Systems, San Jose, CA 95134 USA (e-mail: jbovingt@cisco.com; sromerog@cisco.com; dsiriani@cisco.com).

Color versions of one or more of the figures in this article are available online at http://ieeexplore.ieee.org.

Digital Object Identifier 10.1109/JSTQE.2019.2945979

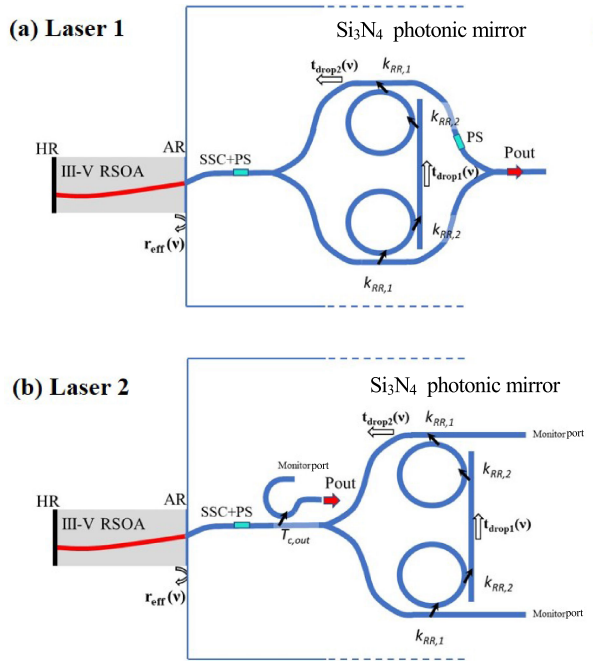

Fig. 1. Sketch of the two III-V/SiN hybrid external-cavity laser structures considered in this paper: (a) *Laser 1* is the configuration with output port from the MZI; (b) in *Laser 2* the output power is taken from the additional coupler inserted before the MZI splitter. The symbols are defined in the text.

TABLE I
HYBRID LASER PARAMETERS

Definition	Symbol and Value
SOA parameters	
Facet high reflection (HR) coefficient	R_{HR}=0.9
Internal quantum efficiency	$\eta_i = 0.76$
Length	$L_{SOA} = 1\,mm$
Active medium volume	$V = 1.5 \cdot 10^{-16} m^{-3}$
Group refractive index	$n_{SOA} = 3.8$
Internal loss	$\alpha_i = 7.6\,cm^{-1}$
Linewidth enhancement factor	$\alpha_H = 3$
Carrier lifetime	$\tau_e = 1\,ns$
Differential gain	$G \cdot n_{SOA}/c = 8.5 \cdot 10^{-17}\,cm^2$
Spontaneous emission factor	$\beta_{sp} = 10^{-4}$
Radiative efficiency	$\eta_r = 0.8$
Optical confinement factor	$\Gamma_c = 0.032$
SiPh mirror parameters	
SSC insetion loss	2 dB
Waveguide group refractive index	$n_{SiN} = 1.76$
Waveguide loss	$0.02\,cm^{-1}$
Bent waveguide loss	$0.04\,cm^{-1}$

reported in literature and the idea at the basis of the design of narrow optical linewidth lasers has not been exploited for the improvement of their tolerance to the optical feedback.

Here we focus on an hybrid laser design similar to those presented in [21] and [18], and we demonstrate that these architectures:

1) are more tolerant to optical feedback because of the longer effective cavity length compared to monolithic conventional single mode semiconductor lasers emitting the same output power with the same WPE
2) are tolerant to very high optical feedback, but at the cost of reduced WPE (ie: lasers tolerant to high spurious optical feedback levels can be designed only accepting very low WPE)
3) can be optimized such that WPE of 18% and laser stability up to -19 dB of external back reflection can be achieved even using commercial MQW III-V SOA

The paper is organized as follows: in Sections II-A and II-B we detail our design method based on simple analytical expressions derived by textbook semiconductor laser rate-equations [22] and by the well known Lang-Kobayashi model [23] adapted at the hybrid laser case. In Section II-C we discuss our results and select the designs that optimize both WPE and feedback tolerance. These designs are then validated in Section III with numerical simulations. In Section IV we draw our conclusions.

II. HYBRID LASER DESIGN

The two types of III-V/SiN hybrid external cavity laser structures considered in this work are shown in Fig. 1 and implemented in a SiN platform. The laser external mirror in Fig. 1(a) is based on a Mach-Zehnder Interferometric (MZI) mirror loaded by two rings providing the narrow band reflection and the Vernier tuning [18], the output power P_{out} is collected at the MZI output. The structure in Fig. 1(b) differs for the presence of the coupler added to extract the output power before the MZI splitter. We define *Laser 1* the structures in Fig. 1(a) and *Laser 2* the configuration in Fig. 1(b). Our aim is finding the best design of *Laser 1* and *Laser 2* that guarantees simultaneously high WPE and tolerance to spurious back reflections (also referred as *optical feedback* in the rest of the paper). We will then compare the two best designs of *Laser 1* and *Laser 2*. Table I reports the parameters we consider for the III-V RSOA of length L_{SOA} and the external mirror based on a SiN platform. The RSOA parameters are taken from experimental characterizations (ie: gain versus current, internal loss, internal quantum efficiency ...) or from typical values of III-V semiconductor materials reported in textbooks [22] (ie: carrier lifetime, linewidth enhancement factor, radiative efficiency, spontaneous emission factor ...). The parameters of the SiN waveguide are given by a foundry.

For *Laser 1* the parameters considered for design optimization are the ring power coupling coefficients k_{RR1} and k_{RR2} (see Fig. 1(a)), that need to be in the under-coupled regime ($k_{RR1} < k_{RR2}$) to give a non null output port transmission coefficient at the ring resonant frequency. This transmission coefficient can be designed via the ratio k_{RR2}/k_{RR1}. In *Laser 2* the parameters are $k_{RR1} = k_{RR2}$ as in the critical coupling regime for maximum mirror reflection and zero transmission, and the output coupler coefficient $T_{c,out}$ (see Fig. 1(b)). In both cases these control parameters define a $2D$ design parameter space which influences the laser performance such as threshold current, output power, WPE, tolerance to optical feedback and small signal intensity modulation response (ie: frequency of the relaxation oscillation and damping factor). The ring radii ($R1$ and $R2$) are chosen to maximize the tuning range and minimize the overlap of the ring resonance peaks adjacent to the lasing one. Specifically, to suppress sufficiently the reflectivity side lobes, we guarantee a separation of twice the FWHM (of the ring resonance) between

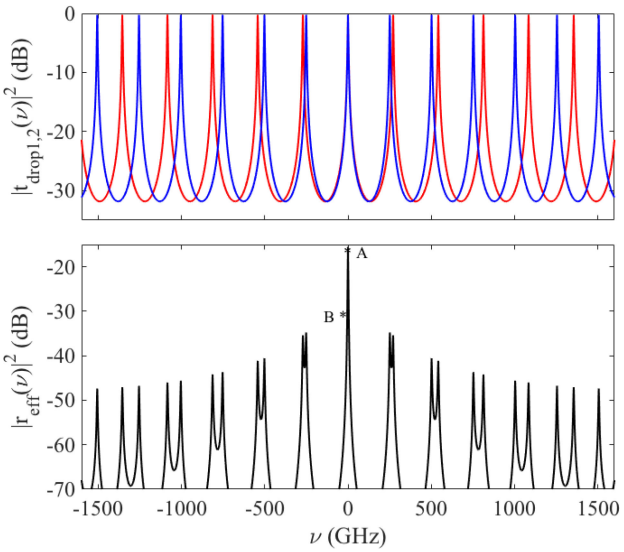

Fig. 2. Example of application of the Vernier principle of *Laser 2* that provides a narrow band effective reflectivity $|r_{eff}(\nu)|^2$ shown in thick black line in the bottom panel. The red and blue lines in the upper panel are the drop transmission coefficients $t_{drop,1}$ and $t_{drop,2}$ of the two rings.

the two ring resonance peaks adjacent to the overlapped ones see for example Fig. 2(a). Based on this criteria it follows that for *Laser 1*, with $k_{RR1} = 0.03$ and $k_{RR2} = 0.32$, we can select $R1 = 107$ μm and $R2 = 95$ μm to guarantee the maximum tuning range of about 27 nm. Whereas for *Laser 2* when $k_{RR1} = k_{RR2} = 0.03$ we select $R1 = 97\mu$m and $R2 = 95\mu$m that leads to a tuning range of more than 150 nm. The maximum tuning range of *Laser 2* is larger than the one of *Laser 1* because the critical coupling of the rings of *Laser 2* gives smaller FWHM and the two radii can be selected closer. The achievable tuning range in *Laser 2* is thus limited only by the SOA gain bandwidth.

In order to compare the various laser configurations in the $2D$ design parameter space, we fix a target power ($P_{out,target}$) at the waveguide output port and we compare the laser performance of the different designs targeting this output power. We will show that the same value of $P_{out,target}$ can be found for different couples of parameters (ie: k_{RR1} and k_{RR2} for *Laser 1*; $k_{RR1} = k_{RR2}$ and $T_{c,out}$ for *Laser 2*): some couples optimize the WPE while reducing the tolerance to optical feedback; other couples can guarantee high laser stability respect to optical feedback, but at the expense of a significant reduction of the WPE. We will however demonstrate the possibility to find a good trade off able to guarantee a WPE of 18% while maintaining the laser stable up to -19 dB of external optical feedback.

A. Calculation of Laser WPE

We define $r_{eff}(\nu)$ the optical electric field effective reflectivity, as function of field frequency ν, of the SiPh mirror at the SOA AR facet (see Fig. 1). As an example we plot in Fig. 2(b) the modulus square of $r_{eff}(\nu)$ and the drop transmission coefficients of the two rings ($t_{drop,1}$ and $t_{drop,2}$) when the latter are tuned to have aligned resonances at the frequency ν_0 corresponding to the wavelength $\lambda_0 = 1.31$ μm. These are calculated by cascading the transmission matrix of the various blocks of the silicon mirror shown in Fig. 1, i.e. the spot-size-converter (SSC), the phase control Section (PS), the MZI splitter, the ring add-drop transmission and output coupler. In the following we assume that the PS Section can fine tune the position of the cavity longitudinal modes respect to the reflectivity peak at ν_0. The lasing longitudinal modes can be tuned at the frequency ν_0 (marked with letter A in Fig. 2(b)) or at the frequency where the derivative of $|r_{eff}(\nu)|$ is positive and maximum (marked with letter B in Fig. 2(b)). We observe that the latter also corresponds to the operating condition that minimizes the laser linewidth [21]. In this work we assume the lasing mode is tuned in point A of Fig. 2(b).

According to the standard laser diode rate-equations approach [22], the III-V SOA bias current ($I_{bias,SOA}$) required to reach $P_{out,target}$ is:

$$I_{bias,SOA} = \left[\frac{P_{out,target}}{\eta_i I_{th}} \frac{e}{\hbar\omega_0} \frac{\alpha_i + \alpha_m}{\alpha_m} \cdot \frac{\left(1 - R_{HR} + \sqrt{\frac{R_{HR}}{|r_{eff}(\nu_0)|^2}}\right)\left(1 - |r_{eff}(\nu_0)|^2\right)}{|t_{eff,out}(\nu_0)|^2} + 1 \right] I_{th} \tag{1}$$

where $\hbar\omega_0 = h\nu_0$ is the recombination energy, α_i is the SOA internal modal loss, α_m is the mirror loss calculated as $\alpha_m = \frac{1}{L_{SOA}} \log\left(\frac{1}{\sqrt{R_{HR}|r_{eff}(\nu_0)|^2}}\right)$, R_{HR} is the SOA HR facet power reflection coefficient, $t_{eff,out}$ is the field transmission coefficient from the SOA AR facet to the output port and η_i is the SOA internal quantum efficiency. The threshold current I_{th} is found as the current when SOA modal gain $g_{mod}(I_{bias,SOA})$ is equal to the total losses $\alpha_i + \alpha_m$; the function $g_{mod}(I_{bias,SOA})$ is provided by measured gain curves of the SOA considered.

The laser WPE at current $I_{bias,SOA}$, defined as the ratio between optical power out and electrical power in, is:

$$WPE = \frac{P_{out,target}}{I_{bias,SOA} \cdot V_{bias}}$$

where the bias voltage V_{bias} is obtained from measured V-I characteristics of the RSOA.

We define the optical energy stored in the hybrid laser cavity (E_{OS}) as the total number of photons times the photon energy; it is given by:

$$E_{OS} = \frac{\hbar\omega}{q} \frac{(I_{bias} - I_{th})}{v_{SOA}(\alpha_m + \alpha_i)} \tag{2}$$

where v_{SOA} is the group velocity in the SOA section. Substituting in the Eq. (2) the expression of the bias current of Eq. (1), we see that at fixed $P_{out,target}$ the optical energy stored depends primarily on the mirror design and, as expected, an increase of E_{OS} leads to reduction of the WPE.

B. Calculation of Critical Feedback Level

An important issue for a number of applications is finding the maximum external feedback level that maintains stable the CW

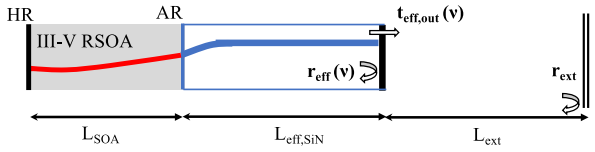

Fig. 3. Effective cavity configuration of the hybrid lasers including external optical feedback.

single mode emission of the hybrid laser with characteristics similar to the one of the solitary (i.e without feedback) laser. We define this external feedback level as the critical feedback level and we indicate it with $R_{ext,critical}$. In order to guarantee a good tolerance to the optical feedback, this level should be as high as possible. Actually the value of $R_{ext,critical}$ is determined by two constraints:

1) the value of the external reflectivity R_{ext} that makes the laser unstable due to undamped relaxation oscillations as predicted by the well known Lang-Kobayashi (LK) model [23]; we denote this value as $R_{ext,LK}$
2) the maximum value R_{ext} that can still be considered a slight perturbation of the hybrid laser cavity; we denote this value as $R_{ext,\max}$. In particular, assuming reasonably that $R_{ext,eff} \leq \frac{|r_{eff}(\nu_0)|^2}{10}$, where $R_{ext,eff} = R_{ext} \cdot |t_{eff,out}(\nu_0)|^4$ is the external mirror reflection as seen from the AR facet of the SOA, it follows:

$$R_{ext} \leq R_{ext,\max} = \frac{|r_{eff}(\nu_0)|^2}{10 \cdot |t_{eff,out}(\nu_0)|^4} \tag{3}$$

If condition (3) is not fulfilled, the LK approach is no longer valid since the laser with optical feedback can be considered as formed by two coupled cavities and the lasing characteristics will be significantly modified by R_{ext}. This limit is relevant because, with the aim of maximizing the optical output power, we can find configurations where $R_{ext,\max}$ is quite low due to a significant increase of $|t_{eff,out}(\nu_0)|$.

To find an approximate analytical expression of $R_{ext,LK}$ determining what we call the LK limit, we model the hybrid laser of Fig. 1 as an effective cavity configuration [22] (see Fig. 3) composed by the active region of the SOA and a passive Section of length $L_{eff,SiN}$ [22], where $L_{eff,SiN}$ is the SiPh mirror effective length calculated as:

$$L_{eff,SiN} = -\frac{v_{g,SiN}}{4\pi} \cdot \frac{\partial \phi_{eff}(\nu)}{\partial \nu}_{|\nu=\nu_0}$$

where $\phi_{eff}(\nu)$ is the phase of the complex reflectivity $r_{eff}(\nu)$ and $v_{g,SiN} = c/n_{SiN}$ the group velocity in the SiPh waveguide. This effective length accounts not only for the effective length of the rings but also for the length of the MZI arms between the splitter and the rings, the length of straight waveguide coupling the two rings and the length of the straight waveguide between the SSC and the MZI splitter. In the results we present in this work these are 493 μm, 300 μm and 200 μm respectively. Total loss (due to waveguide loss, ring loss, transmission coefficients etc...) are accounted by the transmission coefficient $t_{eff,out}(\nu_0)$ at the output facet and calculated as cascade of transmission matrices of the blocks of the SiPh mirror. As shown in Fig. 3, the external optical feedback is represented as a concentrated additional back reflection r_{ext} located at the distance L_{ext} respect to the effective laser output.

The effective LK equation takes the form [23] :

$$\frac{dE(t)}{dt} = \frac{1}{2}\left[G_{eff}(N(t)-N_0) - \frac{1}{\tau_{p,eff}}\right]E(t) + \frac{k}{\tau_{in,eff}}E(t-\tau)cos(\omega_0\tau + \phi(t) - \phi(t-\tau)) \tag{4}$$

$$\frac{d\phi(t)}{dt} = \frac{1}{2}\alpha_H\left[G_{eff}(N(t)-N_0) - \frac{1}{\tau_{p,eff}}\right] - \frac{k}{\tau_{in,eff}}\frac{E(t-\tau)}{E(t)}sin(\omega_0\tau + \phi(t) - \phi(t-\tau)) \tag{5}$$

$$\frac{dN(t)}{dt} = \frac{\eta_i I_{bias,SOA}}{eV} - \frac{N(t)}{\tau_e} - \frac{G_{eff}}{\Gamma_c}(N(t)-N_0)|E(t)|^2 \tag{6}$$

where $E(t)$, $\phi(t)$ are the intensity and phase of the slowly time varying electric field and $N(t)$ is the carrier density in the gain section. We assume a linear gain model for the variation of gain respect to carrier density close to the transparency value N_0; the SOA modal gain is therefore $g_{mod}(N) = \frac{G}{v_{SOA}} \cdot (N(t) - N_0)$. For sake of simplicity non linear effects such as gain compression as well as thermal effects that may both limit the maximum output power have not been considered in the model. The effective differential gain is:

$$G_{eff} = G\frac{v_{eff}}{v_{SOA}} \tag{7}$$

being v_{eff} the group velocity in the effective cavity :

$$v_{eff} = c\frac{L_{SOA} + L_{eff,SiN}}{L_{SOA} \cdot n_{SOA} + L_{eff,SiN} \cdot n_{SiN}}.$$

The quantity:

$$\frac{1}{\tau_{p,eff}} = v_{eff}\left(\alpha_m + \alpha_i\right)$$

is the effective photon lifetime, and

$$\tau_{in,eff} = \frac{2}{c}(n_{SOA} \cdot L_{SOA} + L_{eff,SiN} \cdot n_{SiN})$$

is the round trip time in the effective laser cavity. Moreover V is the active medium volume, τ_e is the carrier life-time and Γ_c is the optical confinement factor in active region of the SOA.

The external optical feedback parameters are the feedback strength:

$$k = \frac{|t_{eff,out}(\nu_o)|^2}{|r_{eff}(\nu_o)|}|r_{ext}|$$

and the external cavity delay $\tau = 2L_{ext}/v_{g,SiN}$.

To consider the worst case, we calculate the critical feedback strength k_c in the so called long cavity limit defined by the

condition $\tau\omega_R/2\pi >> 1$, where ω_R is the relaxation oscillation angular frequency at the current $I_{bias,SOA}$ [22]. In this long cavity limit the laser instability is also independent on the phase of the optical feedback. The critical feedback strength k_c is therefore the minimum value of k beyond which the CW laser emission becomes unstable triggered by undamped relaxation oscillations [23]. It is given by the expression [24]:

$$k_c = \frac{\Gamma_{R,eff}\tau_{in,eff}}{2\alpha_H^2} \cdot \sqrt{1+\alpha_H^2} \tag{8}$$

where Γ_R is the damping factor of the hybrid laser relaxation oscillations:

$$\Gamma_{R,eff} = \frac{1}{\tau_e} + \frac{G}{v_{SOA}} \frac{1}{\alpha_m + \alpha_i} \frac{\eta_i (I_{bias,SOA} - I_{th})}{qV} \tag{9}$$

The corresponding optical linewidth is:

$$\Delta\nu = \beta_{sp} v_{SOA} (\alpha_m + \alpha_i) \frac{\eta_r I_{th}}{(I_{bias,SOA} - I_{th})} \frac{(1+\alpha_H)^2}{4\pi} \cdot \left(\frac{n_{SOA} \cdot L_{SOA}}{n_{SOA} \cdot LSOA + n_{SiN} \cdot L_{eff,SiN}} \right)^2 \tag{10}$$

where β_{sp} is the spontaneous emission factor and η_r is the radiative efficiency.

Substituting in Eq. (9) and (10) the expression of the bias current $I_{bias,SOA}$ of eq. (1), we see the damping factor and the linewidth depends on the target output power and, at fixed $P_{out,target}$, they can be optimized by the mirror design.

For a fixed $P_{out,target}$ and from Eqs. (8), (1) and (2), it derives that the critical feedback level can be increased by either increasing the damping factor Γ_R (via a decrease of the mirror loss that leads to the increase of the optical energy stored E_{OS} with reduction of WPE) or by increasing the effective round trip time $\tau_{in,eff}$ via an increase of $L_{eff,SiN}$.

Similarly, from Eqs. (10), (1) and (2), the optical linewidth at fixed $P_{out,target}$ is reduced either increasing E_{OS} or increasing $L_{eff,SiN}$. Thus we conclude that the optimization of the tolerance to optical feedback also leads to the optimization of the laser linewidth and viceversa. These design concepts are further detailed in the next section reporting the design results.

From the expression of the feedback strength k we can then calculate the maximum value of R_{ext} tolerated from a stable CW hybrid laser as predicted by LK model:

$$R_{ext,LK} = \frac{k_c^2 \cdot |r_{eff}(\nu_0)|^2}{|t_{eff,out}(\nu_0)|^4}.$$

Finally the maximum tolerated feedback level is obtained as the minimum of the two constrains:

$$R_{ext,critical} = \min\left\{ R_{ext,\max}, R_{ext,LK} \right\} \tag{11}$$

C. Design Results

In this section we report the design (based on the simple expressions of the previous section) of *Laser 1* and *Laser 2* with the goal of finding a good trade off between a high WPE and feedback tolerance at a given target output power. Our conclusions will be then validated in Section III via numerical solution of the effective LK equations.

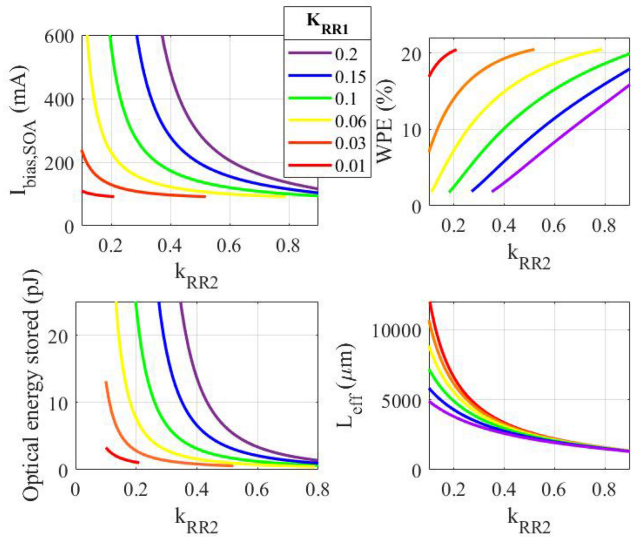

Fig. 4. Solitary laser parameters (SOA bias current, WPE, optical energy stored in the laser cavity E_{OS} and effective length L_{eff}) at $P_{out,target} = 20$ mW as function of the design parameters $k_{RR,1}$ and $k_{RR,2}$ for *Laser 1*.

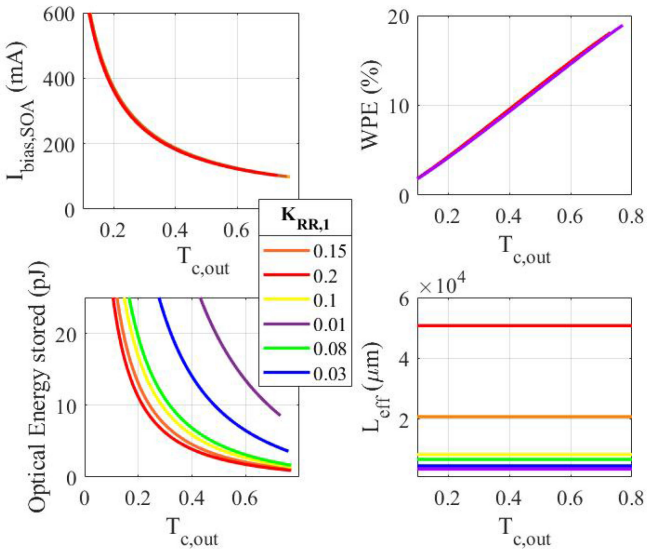

Fig. 5. Solitary laser parameters (SOA bias current, WPE, optical energy stored in the laser cavity E_{OS} and effective length L_{eff}) at $P_{out,target} = 20$ mW as function of the design parameters $k_{RR,1} = k_{RR,2}$ and $T_{c,out}$ for *Laser 2*.

Fig. 4 plots the performance of *Laser 1* with $R_{ext} = 0$ (solitary laser) for target output power $P_{out,target} = 20$ mW. We show the SOA bias current, the corresponding WPE, the optical energy stored, E_{OS}, and the SiPh mirror effective length as function of k_{RR1} and k_{RR2}. The same characteristics are plotted as function of $k_{RR2} = k_{RR1}$ and $T_{c,out}$ for *Laser 2* in Fig. 5. As anticipated, the performance of *Laser 1* is very sensitive to both k_{RR1} and k_{RR2}; as a general trend we see that, for a fixed value of k_{RR1}, the increase of k_{RR2} leads to a reduction of SOA bias current with an increase of WPE because of the increase of $|t_{eff,out}|$; the energy stored in the cavity as consequence reduces. On the contrary, for decreasing values of k_{RR2} (i.e. $k_{RR2} < 0.4$) we see an increase of both E_{OS} and $L_{eff,SiN}$ with a consequent increase of the critical feedback level according to

Eq. (8). In this range, for a fixed value of k_{RR2}, the effective length, the WPE and the energy stored can be designed with a proper choice of k_{RR1}: reducing k_{RR1} the effective length increases (the longest is about 1 cm with $k_{RR1} = 0.01$ and $k_{RR2} = 0.1$) and also the WPE can be maximized, but at the cost of a low E_{OS}. The maximum WPE is 20% with $k_{RR1} = 0.01$ and $k_{RR2} = 0.2$.

From Fig. 5 we notice that the SOA bias current and WPE of *Laser 2* are almost independent on $k_{RR1} = k_{RR2}$ because $|t_{eff,out}|$ is determined by $T_{c,out}$; the slight dependence with k_{RR1} of the optical energy stored is due to the different threshold currents caused by higher loss in the high Q rings obtained with low values of $k_{RR1} = k_{RR2}$. The high-Q design of the ring is however crucial for designing long $L_{eff,SiN}$ and therefore to increase the critical feedback level k_c. At the maximum WPE of 19% it is feasible to maximize the effective length reaching the value of 5 cm with $k_{RR1} = k_{RR2} = 0.01$.

Based on Fig. 4 and Eq. (8), we thus conclude that the design parameters of *Laser 1* can be chosen to maximize WPE (via a reduction of $I_{bias,SOA}$ and E_{OS}) at the expense of a low k_c or, on the contrary, to maximize the critical feedback level k_c at the expense of low WPE (because of high $I_{bias,SOA}$ and E_{OS}). In general we need to pay in terms of electrical power the high tolerance to the optical feedback requested for isolator free applications. Similar considerations are valid also for the minimization of the laser linewidth since it shares similar dependence on the $L_{eff,SiN}$ and bias current.

In *Laser 1* the design with high WPE and long $L_{eff,SiN}$ is only possible with very different k_{RR2} and k_{RR1} staying in a ratio of about 10 as for example the red curve in Fig. 4(b).

The structure of *Laser 2* relaxes this requirement a bit since Fig. 5 shows that we can select a design with high WPE (determined almost by $T_{c,out}$) and control the effective length, and thus the critical feedback level, via the choice of $k_{RR1} = k_{RR2}$.

These conclusions are further validated by the results reported in Fig. 6, where we plot the maximum external reflectivity $R_{ext,critical}$ as function of the WPE for both lasers and for different values of k_{RR1}. In general we see that an increase of WPE is always accompanied by a reduction $R_{ext,critical}$. The dashed lines, reporting the LK limit, tell us that at low WPE, when high photon density is accumulated in the cavity and/or long $L_{eff,SiN}$ is possible, the laser would be able to tolerate very high external optical feedback and thus $R_{ext,critical}$ is limited by $R_{ext,\max}$ given by Eq. (3). Increasing WPE the angular point of each solid lines indicates the transition from the limit imposed by $R_{ext,\max}$ to the LK limit.

The optical linewidth calculated according to Eq. (10) is also plotted in Fig. 7. The trends are very similar to those reported in Fig. 6 for the critical feedback level: the linewidth increases as WPE increases and those designs with longer effective length allows for smaller linewidth; as consequence Laser 2 allows for smaller linewidth respect to *Laser 1*. As an example we compare in Fig. 8 and Fig. 9 the designs of *Laser 1* and *Laser 2* emitting both $P_{out,target} = 20$ mW with $WPE = 18\%$. From Fig. 8(a) we see that all couples k_{RR2} and k_{RR1} of *Laser 1* staying in the ratio determined by the blue dashed curve satisfy the requirement $P_{out,target} = 20$ mW with $WPE = 18\%$; k_{RR2}/k_{RR1} varies

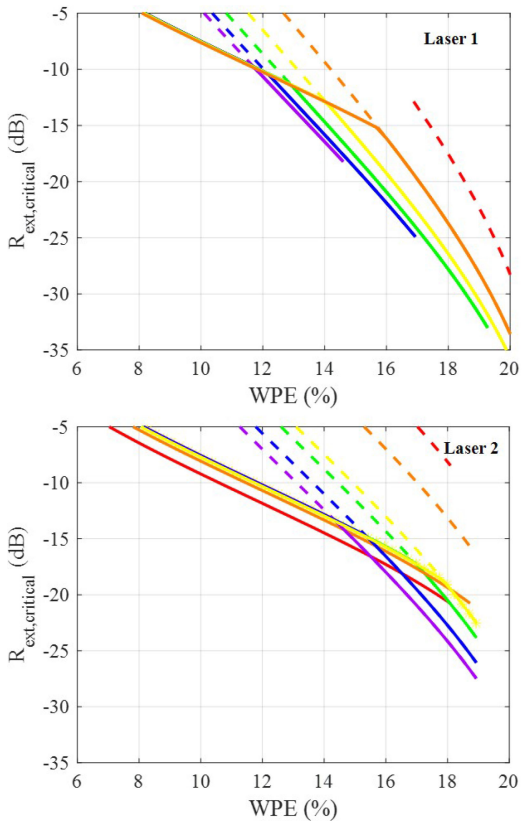

Fig. 6. Critical feedback level $R_{ext,critical}$ as function of the WPE of *Laser 1* and *Laser 2* (colors are the same as in Fig. 4 and Fig. 5). Dashed line is the LK limit $R_{ext,LK}$, whereas solid line is the limit according to Eq. (11).

between 12 and 7. On the contrary, for *Laser 2*, the ratio k_{RR2}/k_{RR1} is always fixed to 1 (red dashed line) and $T_{c,out}$ is fixed to 0.73 to get $P_{out,target} = 20$ mW with $WPE = 18\%$. The corresponding effective lengths of both lasers are shown in Fig. 8(a) as solid curves: the maximum effective length of *Laser 2* is about 5 times longer then that of *Laser 1*. Since both lasers give same WPE and output power, their SOA bias current and optical energy stored are only slightly dependent on the laser configuration and, for the same configuration (ie: *Laser 1* or *Laser 2*) these parameters are slightly dependent on k_{RR2}. Therefore the damping factors in Fig. 8(b) change with k_{RR2} of a factor 1.2 and 1.1 for *Laser 1* and *Laser 2* respectively. On the other hand, the effective length in Fig. 8(a) can change of a factor 7.7 and 15 for *Laser 1* and *Laser 2* respectively. For *Laser 1*, the resulting $R_{ext,LK}$ in solid line of Fig. 9 can therefore be between -17 dB and -29 dB by the design of k_{RR2} and the corresponding ratio k_{RR2}/k_{RR1} given by Fig. 8(a). For *Laser 2*, $R_{ext,LK}$ stays between -9 dB and -24 dB. However, for both *Laser 1* and *Laser 2* the maximum external reflection is limited by $R_{ext,\max}$ of -19 dB indicated by the dashed line of Fig. 9.

It is important to observe that our design method starts by fixing the target output power $P_{out,target}$ which is defined by the specific applications. We have observed that when $P_{out,target}$ increases respect to the 20 mW set here the $R_{ext,critical}$ of Fig. 9 scales as the square of the output power as consequence of the increase of the optical energy stored in the cavity. On the

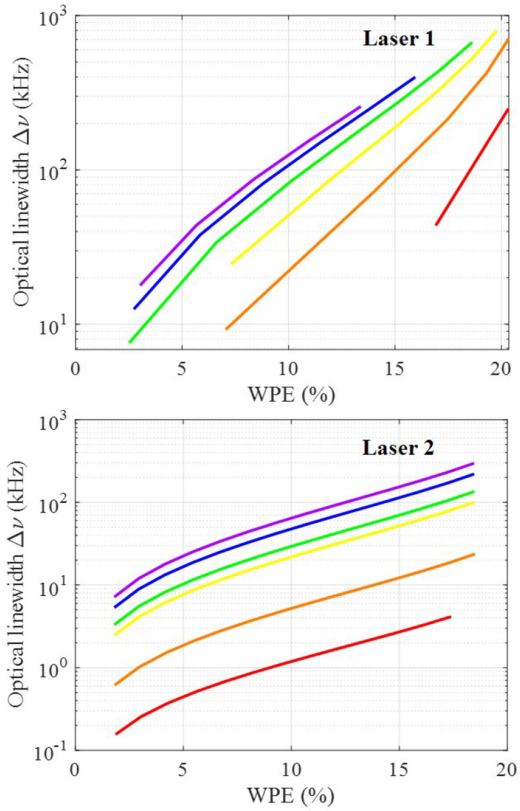

Fig. 7. Optical linewidth $\Delta\nu$ as function of the WPE of *Laser 1* and *Laser 2* (colors are the same as in Fig. 4 and Fig. 5).

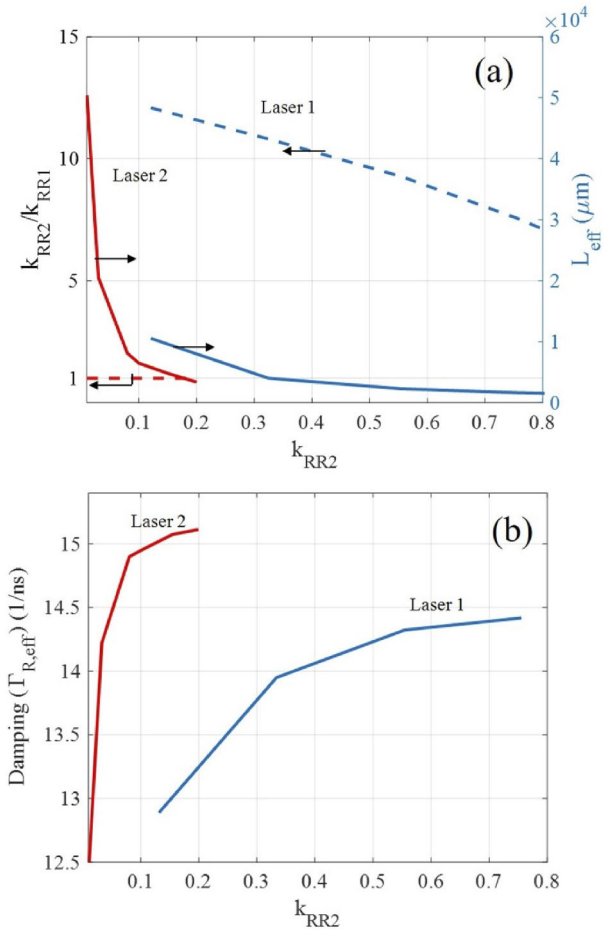

Fig. 8. Design parameters for $P_{out,target} = 20$ mW with $WPE = 18\%$. The ratio k_{RR2}/k_{RR1} in dashed line and corresponding L_{eff} in solid line are reported in panel (a), while the damping factors are shown in panel (b). For *Laser 2* and based on Fig. 5(b), we have chosen $T_{c,out} = 0.73$.

contrary, when the target output power is very low (just a few milliwatts), the design procedure finds solutions with much low WPE (a few percents) but critical feedback levels comparable to those reported in Fig. 9.

III. Numerical Simulations

In order to check the validity of the results in Fig. 9 and to investigate the laser behaviour beyond the instability threshold R_{extLK}, we have numerically integrated the set of delayed differential equations Eqs. (4)–(6) using the delayed differential equation solver *dde23* in Matlab. We have numerically simulated the designs marked with the letters in the blue and red curves of Fig. 9. As an example of experimentally accessible quantifier of the tolerance of the hybrid laser to optical feedback, we report in Fig. 10 the Relative Intensity Noise (RIN) defined as:

$$RIN = 10\log_{10}\left(\frac{<\delta P(t)^2>}{P_{out,target}^2}\right)$$

where $<\delta P(t)^2>$ is the mean-square of the laser power fluctuation $\delta P(t) = P(t) - P_{out,target}$ around the bias output power $P_{out,target}$. $P(t)$ is calculated as $P(t) = |E(t)|^2 \cdot |t_{eff,out}(\omega_0)|^2$.

The sharp transition from low to high RIN for the different cases does not exactly coincides with $R_{ext,LK}$ reported in Fig. 9. This can be explained by observing that the latter represents an approximation for the minimum tolerated feedback rigorously valid in the long cavity limit $\omega_R/2\pi >> 1$, while in all our numerical simulations we have considered the value of $L_{ext} = 5$ cm that gives $\omega_R/2\pi = 6$. For comparison, with black line in Fig. 10 we also show the RIN associated to a monolithic single mode laser (i.e. with $L_{eff,SiN} = 0$) with the same $WPE = 18\%$ and target output power of $P_{out,target} = 20$ mW. The latter turns out to be by far less tolerant to the optical feedback than the hybrid laser designs and in particular a difference of about 13 dB is observed with respect to the maximum acceptable feedback set by the dashed line corresponding to $R_{ext,\max} = -19$ dB in Fig. 9. Up to $R_{ext,\max} = -19$ dB we can also see that designs $E2$ and $F2$ are always stable. As an example we show in Fig. 11 the bifurcation diagram for the design $D2$ obtained by plotting the local maxima and minima in the output power temporal trace for increasing value of the external feedback. A transition from the CW operation (region A) to a steady state characterised by regular oscillations at the free running relaxation frequency (region B) is first observed at $R_{ext} = -18$ dB followed by a route to chaos for higher feedback levels (region C) where the beating between external cavity modes also might take part in ruling the laser dynamics. In the inset of Fig. 11 we report the time trace for $R_{ext} = -18$ dB and the corresponding power spectrum where the main peak at about $\approx \omega_R/2\pi$ is highlighted. Also lines, approximately spaced of the

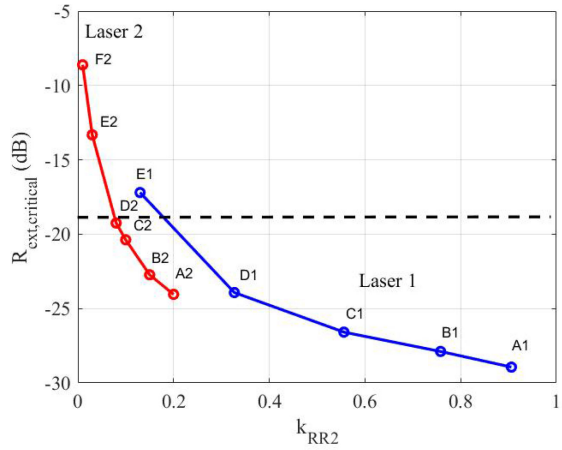

Fig. 9. Maximum external reflectivity associated with the LK limit ($R_{ext,LK}$) at $P_{out,target} = 20$ mW with $WPE = 18\%$ in solid line; the dashed line is $R_{ext,\max}$. The curves are calculated for the same design parameters of Fig. 8.

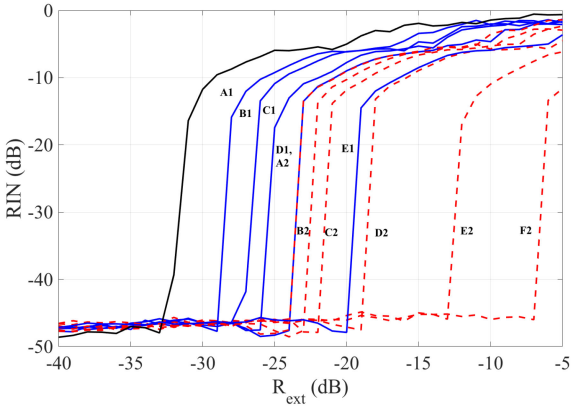

Fig. 10. Calculated RIN versus R_{ext} for the designs marked with the letters on the blue and red curves of Fig. 9. The solid black line is the case where we impose $L_{eff,SiN} = 0$ while keeping $P_{out,target} = 20$ mW with $WPE = 18\%$.

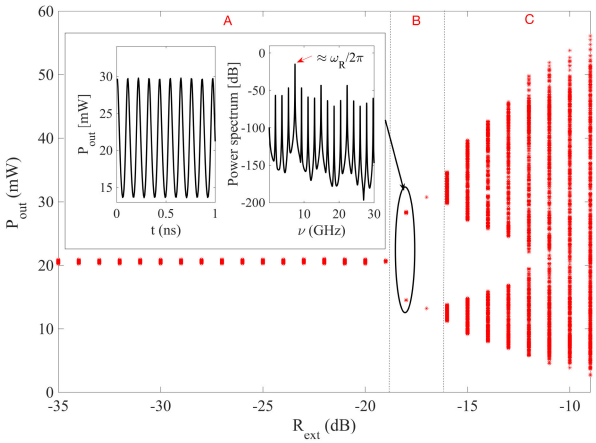

Fig. 11. Bifurcation diagram showing the transition from CW operation (region A) to a regime of periodic oscillations at about the solitary laser relaxation frequency $\approx \omega_R/2\pi$ (region B) of *Laser 2*, design $D2$. For higher feedback the system shows a route to a chaotic dynamics (region C). In the inset the temporal trace and the corresponding power spectrum are shown for the value $R_{ext} = -18$ dB that falls in region B.

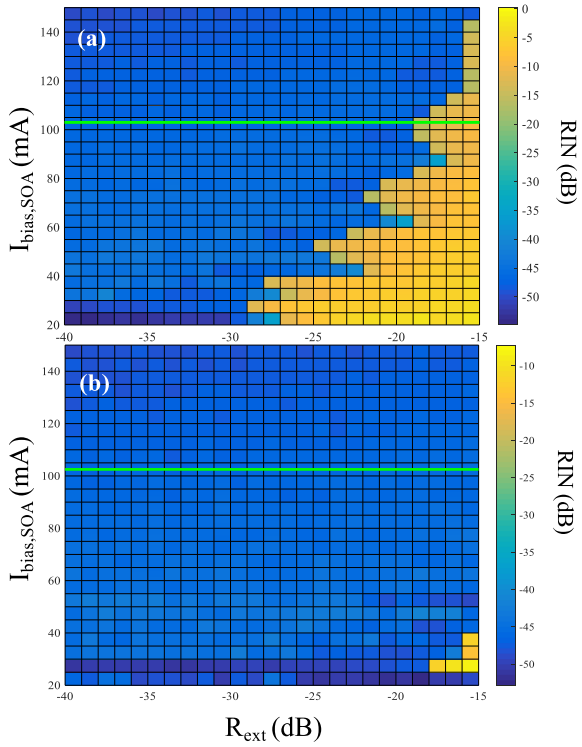

Fig. 12. RIN map obtained by scanning the external reflectivity R_{ext} and the bias current $I_{bias,SOA}$ for the *Laser 2* structure corresponding to the design point $D2$ (a) and the design point $F2$ (b).

external cavity free spectral range $c/2n_{SiN}L_{ext} = 1.7$ GHz, are distinguishable although strongly damped.

Finally for the more stable designs of *Laser 2* corresponding to point $D2$, for which $R_{ext,critical} = R_{ext,LK}$, and to point $F2$, for which $R_{ext,critical} = R_{ext,\max}$, we show in Fig. 12 the map of the simulated RIN for different values of the R_{ext} and SOA bias currents $I_{bias,SOA}$. The cuts along the green line correspond to the RIN reported in Fig. 10. Referring to Fig. 12(a), for design $D2$ and lower bias current (i.e. lower photon density) we observe a shift of the instability threshold towards lower values of R_{ext} whereas the feedback tolerance improves at higher currents. We verified that the stability tongues in the region of low bias current (i.e.: around 45 mA and 60 mA) occur when the quantity $\omega_R\tau/2\pi$ is a small integer and the relaxation oscillations are more damped [25]. Interestingly, for the design $F2$ the RIN remains very low for almost all the considered values of $I_{bias,SOA}$ thus indicating ultra stable CW emission.

IV. Conclusion

In conclusion we report on two possible configurations of a tunable hybrid laser based on III-V active medium and SiN mirror. For a target output power of 20 mW we compare different designs adopting as a figure of merit their WPE and tolerance respect to spurious back reflections. The latter, coming from the several interfaces present in the SiPh PICor from the output coupling fiber, might detrimentally affect the stability of the hybrid lasers CW emission and consequently limit their use in

many relevant datacom applications. The effects of unwanted optical feedback is studied in the framework of an effective Lang-Kobayashi model through both steady state and dynamical simulations. Although it turns out that is not possible to simultaneously maximixe WPE and robustness with respect to feedback, in analogy to what happen when looking for an efficient and at the same time narrow linewidth hybrid laser, we demonstrate that keeping fixed the WPE it is possible to increase the feedback insensitivity by increasing the effective length of the photonic mirror. In this regard our hybrid laser design named *Laser 2*, where light is extracted by a coupler placed before the MZI splitter, turns out to be more robust to perturbations induced by optical feedback. Following this evidence we were able to find an optimal design that represents a very good trade off trade off between a high WPE (up to 18%) and laser stability (up to -19 dB).

ACKNOWLEDGMENT

The authors would like to thank Dr. Fabrizio Forghieri (Cisco Systems, Italy) for the stimulating discussions.

REFERENCES

[1] D. Thomson *et al.*, "Roadmap on silicon photonics," *J. Opt.*, vol. 18, no. 7, Jun. 2016, Art. no. 073003. [Online]. Available: https://doi.org/10.1088

[2] Z. Zhou, R. Chen, X. Li, and T. Li, "Development trends in silicon photonics for data centers," *Opt. Fiber Technol.*, vol. 44, pp. 13–23, 2018. [Online]. Available: http://www.sciencedirect.com/science/article/pii/S1068520017303309

[3] S. Tanaka, S.-H. Jeong, S. Sekiguchi, T. Kurahashi, Y. Tanaka, and K. Morito, "High-output-power, single-wavelength silicon hybrid laser using precise flip-chip bonding technology," *Opt. Express*, vol. 20, no. 27, pp. 28 057–28 069, Dec. 2012. [Online]. Available: http://www.opticsexpress.org/abstract.cfm?URI=oe-20-27-28057

[4] T. Komljenovic *et al.*, "Heterogeneous silicon photonic integrated circuits," *J. Lightw. Technol.*, vol. 34, no. 1, pp. 20–35, Jan. 2016. [Online]. Available: http://jlt.osa.org/abstract.cfm?URI=jlt-34-1-20

[5] A. Y. Liu and J. Bowers, "Photonic integration with epitaxial III–V on silicon," *IEEE J. Sel. Topics Quantum Electron.*, vol. 24, no. 6, Nov./Dec. 2018, Art. no. 6000412.

[6] Y. Shoji, K. Miura, and T. Mizumoto, "Optical nonreciprocal devices based on magneto-optical phase shift in silicon photonics," *J. Opt.*, vol. 18, no. 1, Nov. 2015, Art. no. 013001. [Online]. Available: https://doi.org/10.1088

[7] P. Pintus *et al.*, "Microring-based optical isolator and circulator with integrated electromagnet for silicon photonics," *J. Lightw. Technol.*, vol. 35, no. 8, pp. 1429–1437, Apr. 2017. [Online]. Available: http://jlt.osa.org/abstract.cfm?URI=jlt-35-8-1429

[8] C. R. Doerr, N. Dupuis, and L. Zhang, "Optical isolator using two tandem phase modulators," *Opt. Lett.*, vol. 36, no. 21, pp. 4293–4295, Nov. 2011. [Online]. Available: http://ol.osa.org/abstract.cfm?URI=ol-36-21-4293

[9] N. Hatori, K. Mizutani, S. Jeong, Y. Tanaka, and K. Kurata, "High reflection tolerance of quantum dot distributed feedback lasers for silicon photonics transmitters," in *Proc. IEEE 14th Int. Conf. Group IV Photon.*, Aug. 2017, pp. 105–106.

[10] A. Y. Liu, T. Komljenovic, M. L. Davenport, A. C. Gossard, and J. E. Bowers, "Reflection sensitivity of 1.3 μm quantum dot lasers epitaxially grown on silicon," *Opt. Express*, vol. 25, no. 9, pp. 9535–9543, May 2017. [Online]. Available: http://www.opticsexpress.org/abstract.cfm?URI=oe-25-9-9535

[11] J. Duan *et al.*, "1.3-μm reflection insensitive InAs/GaAs quantum dot lasers directly grown on silicon," *IEEE Photon. Technol. Lett.*, vol. 31, no. 5, pp. 345–348, Mar. 2019.

[12] H. Huang *et al.*, "Analysis of the optical feedback dynamics in InAs/GaAs quantum dot lasers directly grown on silicon," *J. Opt. Soc. Am. B*, vol. 35, no. 11, pp. 2780–2787, Nov. 2018. [Online]. Available: http://josab.osa.org/abstract.cfm?URI=josab-35-11-2780

[13] B. Dong *et al.*, "Influence of the polarization anisotropy on the linewidth enhancement factor and reflection sensitivity of 1.55 um inp-based inas quantum dash lasers," *Appl. Phys. Lett.*, vol. 115, no. 9, 2019, Art. no. 091101.

[14] D. Lenstra, T. T. M. van Schaijk, and K. A. Williams, "Toward a feedback-insensitive semiconductor laser," *IEEE J. Sel. Topics Quantum Electron.*, vol. 25, no. 6, Nov./Dec. 2019, Art. no. 1502113.

[15] N. Kobayashi *et al.*, "Silicon photonic hybrid ring-filter external cavity wavelength tunable lasers," *J. Lightw. Technol.*, vol. 33, no. 6, pp. 1241–1246, Mar. 2015.

[16] J.-H. Lee *et al.*, "Demonstration of 12.2% wall plug efficiency in uncooled single mode external-cavity tunable SI/III–V hybrid laser," *Opt. Express*, vol. 23, no. 9, pp. 12 079–12 088, May 2015. [Online]. Available: http://www.opticsexpress.org/abstract.cfm?URI=oe-23-9-12079

[17] C. G. H. Roeloffzen *et al.*, "Low-loss Si_3N_4 triplex optical waveguides: Technology and applications overview," *IEEE J. Sel. Topics Quantum Electron.*, vol. 24, no. 4, Jul./Aug. 2018, Art. no. 4400321.

[18] H. Guan *et al.*, "Widely-tunable, narrow-linewidth III–V/silicon hybrid external-cavity laser for coherent communication," *Opt. Express*, vol. 26, no. 7, pp. 7920–7933, Apr. 2018. [Online]. Available: http://www.opticsexpress.org/abstract.cfm?URI=oe-26-7-7920

[19] T. Komljenovic *et al.*, "Widely tunable narrow-linewidth monolithically integrated external-cavity semiconductor lasers," *IEEE J. Sel. Topics Quantum Electron.*, vol. 21, no. 6, Nov./Dec. 2015, Art. no. 1501909.

[20] J. L. Zhao *et al.*, "Narrow-linewidth widely tunable hybrid external cavity laser using Si_3N_4/SiO_2 microring resonators," in *Proc. IEEE 13th Int. Conf. Group IV Photon.*, Aug. 2016, pp. 24–25.

[21] Y. Fan *et al.*, "Spectral linewidth analysis of semiconductor hybrid lasers with feedback from an external waveguide resonator circuit," *Opt. Express*, vol. 25, no. 26, pp. 32 767–32 782, Dec. 2017. [Online]. Available: http://www.opticsexpress.org/abstract.cfm?URI=oe-25-26-32767

[22] S. C. L. A. Coldren, *Semiconductor and Photonic Integrated Circuits*. New York, NY, USA: Wiley, 1995.

[23] J. Mork, B. Tromborg, and J. Mark, "Chaos in semiconductor lasers with optical feedback: theory and experiment," *IEEE J. Quantum Electron.*, vol. 28, no. 1, pp. 93–108, Jan. 1992.

[24] J. Helms and K. Petermann, "A simple analytic expression for the stable operation range of laser diodes with optical feedback," *IEEE J. Quantum Electron.*, vol. 26, no. 5, pp. 833–836, May 1990.

[25] D. Lenstra, "Relaxation oscillation dynamics in semiconductor diode lasers with optical feedback," *IEEE Photon. Technol. Lett.*, vol. 25, no. 6, pp. 591–593, Mar. 2013.

Lorenzo Columbo received the M.Sc. degree in physics from the Universitá deli Studi di Bari, Bari, Italy, in 2002 and the Ph.D. degree in physics and astrophysics from the Dipartimento di Scienza e Alta Tecnologia, Universitá degli Studi dell'Insubria, Como, Italy, in 2007. He worked as a Researcher in the field of self-organization phenomena in semiconductor lasers with the Institut Nonlinéaire de Nice, Valbonne, France, Dipartimento di Fisica of the Universitá degli Studi di Bari, Bari, Italy and at the Dipartimento di Scienza e Alta Tecnologia, Universitá degli Studi dell'Insubria, Como, Italy. In April 2016, he joined the Dipartimento di Electronica e Telecomunicazioni of the Politecnico di Torino, Torino, Italy where his theoretical research activity focuses on optical frequency combs generation in single section Quantum Dot lasers and on the modeling of hybrid laser dynamics in silicon photonics platforms. His main fields of interest are quantum electronics, optoelectronics, and nonlinear optics.

Jock Bovington received the bachelor's degrees in physics and electrical engineering (specialization in computer engineering) from Seattle University, Seattle, WA, USA, and the M.S. and Ph.D. degrees in electrical engineering from the University of California Santa Barbara (UCSB), Santa Barbara, CA, USA, as an NSF Graduate Research Fellow. He researched heterogeneous integration of III–V materials with Si and Si_3N_4 waveguide on Si for lasers, including demonstrating the first four wavelength fiber link using this technology as a member of Intel's, Photonic Technology Lab. In 2014, he joined Oracle and demonstrated efficient hybrid III–V/Si lasers and flexible comb laser sources using Si micro-ring mirrors. He is currently working on laser diodes and silicon photonics with Cisco. He has authored or coauthored more than 50 technical journal articles, conference publications, and patents in the area of III–V/Si integration. He was a co-founder and first VP of the IEEE Photonics Society Student Chapter at UCSB.

Sebastian Romero-Garcia was born in Rute, Spain, in 1984. He received the M.Sc. degree in telecommunications engineering from the University of Malaga, Malaga, Spain, in 2009 and the Dr.-Ing. degree from RWTH Aachen University, Aachen, Germany, in 2016. From 2009 to 2012, he was working as a Research Assistant with the Photonics & RF Research Lab, University of Malaga. In 2012, he joined the Institute of Integrated Photonics with RWTH Aachen where he worked on the development of high-performance components for silicon photonics transceivers aimed at datacom applications as well as silicon nitride photonic integrated circuits for biosensors. He is currently a Hardware Engineer with Cisco Optical where he is focusing on the development of transceivers for digital coherent communication systems.

Dominic F. Siriani received the B.S., M.S., and Ph.D. degrees in electrical engineering from the University of Illinois at Urbana-Champaign, Champaign, IL, USA, in 2006, 2007, and 2011, respectively. During his graduate studies, he researched photonic crystal VCSELs and coherently coupled antiguided VCSEL arrays. In 2011, he joined the technical staff with Lincoln Laboratory, Massachusetts Institute of Technology, where he was with the Laser Technology and Applications Group performing research and development on monolithic photonic integrated circuits, high-power laser diodes, quantum cascade lasers, and visible III-nitride photonics. He is currently working on laser diodes and silicon photonics with Cisco Systems, Allentown, PA, USA. He has authored or coauthored more than 50 technical journal articles and conference presentations and a book chapter. He is a member of the Optical Society of America and IEEE/Photonics Society. He is currently serving as an Associate Vice President of Communications for the IEEE Photonics Society.

Mariangela Gioannini received the Laurea degree in electronic engineering and the Ph.D. degree in electronic and communication engineering from Politecnico di Torino, Turin, Italy, in 1998 and 2002, respectively. She is currently an Associate Professor with the Dipartimento di Elettronica e Telecomunicazioni, Politecnico di Torino. Her research interests include modelling of semiconductor lasers, optical amplifiers and superluminescent light-emitting diodes based on quantum dot materials and design of lasers for silicon photonics platform. Other topics of interest are on laser dynamics, with focus on comb lasers, and modelling and design of third generation solar cells.